

Alma Mater Studiorum Università di Bologna  
Archivio istituzionale della ricerca

Frequency Steerable Transducers for Ultrasonic Structural Health Monitoring

This is the final peer-reviewed author's accepted manuscript (postprint) of the following publication:

*Published Version:*

De Marchi L., Mohammadgholiha M., Dibiase M. (2023). Frequency Steerable Transducers for Ultrasonic Structural Health Monitoring. New York : IEEE Computer Society [10.1109/IUS51837.2023.10308261].

*Availability:*

This version is available at: <https://hdl.handle.net/11585/953742> since: 2024-01-23

*Published:*

DOI: <http://doi.org/10.1109/IUS51837.2023.10308261>

*Terms of use:*

Some rights reserved. The terms and conditions for the reuse of this version of the manuscript are specified in the publishing policy. For all terms of use and more information see the publisher's website.

This item was downloaded from IRIS Università di Bologna (<https://cris.unibo.it/>).  
When citing, please refer to the published version.

(Article begins on next page)

This is the final peer-reviewed accepted manuscript of:

L. De Marchi, M. Mohammadgholiha and M. Dibiase, "Frequency Steerable Transducers for Ultrasonic Structural Health Monitoring," 2023 IEEE International Ultrasonics Symposium (IUS), Montreal, QC, Canada, 2023, pp. 1-8.

The final published version is available online at:  
<https://doi.org/10.1109/IUS51837.2023.10308261>

#### Terms of use:

Some rights reserved. The terms and conditions for the reuse of this version of the manuscript are specified in the publishing policy. For all terms of use and more information see the publisher's website.

*This item was downloaded from IRIS Università di Bologna (<https://cris.unibo.it/>)*

***When citing, please refer to the published version.***

# Frequency Steerable Transducers for Ultrasonic Structural Health Monitoring

Luca De Marchi  
DEI - Electrical, Electronic,  
and Information Engineering Dept.  
University of Bologna  
40136 Bologna, Italy  
l.demarchi@unibo.it

Masoud Mohammadgholiha  
DEI - Electrical, Electronic,  
and Information Engineering Dept.  
University of Bologna  
40136 Bologna, Italy  
m.mohammadgholiha@unibo.it

Marco Dibiase  
DEI - Electrical, Electronic,  
and Information Engineering Dept.  
University of Bologna  
40136 Bologna, Italy  
marco.dibiase3@unibo.it

**Abstract**—Ultrasonic Structural Health monitoring systems are typically implemented through phased arrays featuring a large number of piezoelectric transducers. However, the permanent installation of such a large number of transducers could hamper the widespread field deployment of SHM systems. To this aim, a possible solution is in the shaping of the piezoelectric transducer electrodes to achieve the capability of steering the ultrasonic beam by simply controlling the central frequency of the actuated pulse. This solution enables the imaging of large 2D areas by actuating just two differential signals. In this work, some recent realizations of Frequency steerable transducers (FSATs) will be presented, detailing the design, simulation, and experimental characterization strategy and the signal processing techniques which can be applied on the acquired signals. It will be shown that FSATs offer several features, such as inherent hardware directivity, and reduced sidelobes, which are essential in the realization of the next generation of ultrasonic Structural Health Monitoring systems.

**Index Terms**—Structural Health Monitoring, Lamb waves, Piezoelectric transducers.

## I. INTRODUCTION

Lamb waves inspection systems have been thoroughly investigated in recent years [1]. The typical implementations of these systems are based on the usage of large network of piezoelectric transducers operated as phased arrays to steer the ultrasonic beam along multiple directions. The beam steering is achieved through constructive/destructive interference between the multiple emitting/receiving elements of the array. Such procedure is commonly referred to as *beam-forming*. The beampattern of the array can be dynamically altered by using beam-steering techniques such as the *delay-and-sum* algorithm. In the GW SHM context, Deutsch et al. [2] developed a phased-array self-focusing method, by which the delay times are adjusted to focus the beam exactly on the defect. In this context Giurgiutiu and Bao [3] proposed the Embedded Ultrasonic Structural Radar (EUSR) to avoid an heavy and complex multichannel phased excitation equipment. Alternatively, phased-arrays can exploit tomography techniques. Schwartz et al. [4] proposed a tomographic approach

for the structural health monitoring of aircrafts. However, a high computational cost is required by these methods. The beam-steering techniques may be based on the actuation of short-time and broad band pulses but this requires the tackling of the multimodal and dispersive propagation of Lamb waves. Vice-versa monochromatic and single mode signals can be excited, to counteract dispersion. However, long-lasting sinusoidal waves using may implicate reduced radial resolution and ambiguity issues in presence of multiple scatters to be detected.

As anticipated, in order to reduce the mainlobe beam width, phased arrays typically require a large number of sensors [5]. This involves complex wiring and multiplexing circuitry one to control each transducer. Further issues are related to the intensive signal processing and large amounts of recorded data. As conclusion, the phased array solution, due to the large number of requested sensors, the sensors-system weight, the high installation costs, the hardware complexity and the significant computational cost, is often unsuitable for embedded applications, as those required in the aeronautical or aerospace fields.

A possible solution to tackle these limitations is in the shaping of the piezoelectric transducer electrodes to achieve the capability of steering the ultrasonic beam by simply controlling the central frequency of the actuated pulse.

These devices, called Frequency steerable transducers (FSATs), will be reviewed in this paper and it will be shown how the electrode shapes design methodology could be adapted to remove the 180° degrees ambiguity which characterizes the first realizations of the frequency steering concepts [6], and how the concept could be extended to transmit and sense wide band signals.

In the next sections, it will be shown how the shaped transducer may offer several features, such as inherent hardware directivity, and reduced sidelobes, which are essential in the realization of the next generation of ultrasonic Structural Health Monitoring systems.

## II. PIEZOELECTRIC TRANSDUCER MODELING

In thin-wall structures, ultrasonic waves may propagate as Lamb waves. Implicit transcendental equations [7], [8] can

The research was conducted as part of the Guided Waves for Structural Health Monitoring (GW4SHM) project, which is financially supported by the Marie Skłodowska-Curie Actions Innovative Training Network, H2020 (Grant No. 860104).

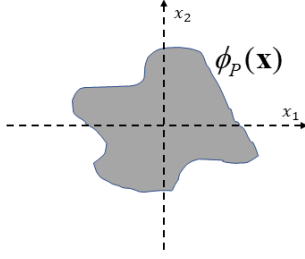


Fig. 1. Model of an arbitrarily shaped piezo-sensor, bonded on the top surface of a thin plate.

be solved numerically to determine a countable infinity of wave-number functions  $k_n(\omega)$  and hence the phase and group velocities of the propagating waves.

Lamb waves can be excited and acquired with different sensing technologies, such as laser and vibrometers. Among these technologies, the one based on the usage of piezoelectric transducers bonded to the inspected structure is very commonly adopted.

The modeling of the transduction effect have been thoroughly investigated by multiple authors and it is briefly reviewed here, following the notation proposed by Senesi and Ruzzene in [9].

In the vast majority of the current applications, piezoelectric transducers come with circular or rectangular shapes, however the adopted model is applicable to arbitrarily shaped sensors, and the results can be extended to the case of transducer used as actuators, on the basis of acoustic reciprocity principles.

The problem at hand is schematically depicted in Fig. 1 where we have a mechanical structure (a thin plate whose area is  $\Omega$ ), and a bonded piezo-sensor of size  $\Omega_P$  and thickness  $t_P$ .

The constitutive equations of a piezoelectric sensor are given by:

$$\begin{cases} \sigma = \mathbf{C}^E \varepsilon - \mathbf{e}^T \mathbf{E} \\ \mathbf{D} = \mathbf{e}^\sigma \varepsilon + \varepsilon^\varepsilon \mathbf{E} \end{cases} \quad (1)$$

where the mechanical stress and strain vectors are given by

$$\begin{aligned} \sigma &= [\sigma_{11}, \sigma_{22}, \sigma_{33}, \tau_{13}, \tau_{23}, \tau_{12}]^T \\ \varepsilon &= [\varepsilon_{11}, \varepsilon_{22}, \varepsilon_{33}, \gamma_{13}, \gamma_{23}, \gamma_{12}]^T \end{aligned} \quad (2)$$

In these equations,  $\mathbf{D}$  and  $\mathbf{E}$  are respectively the electric displacement and the electric field vectors, while  $\mathbf{e}^\sigma$  is the piezo-coupling matrix evaluated at constant stress,  $\varepsilon^\varepsilon$  is the permittivity matrix at constant strain and,  $\mathbf{C}^E$  is the stiffness matrix at constant electric field. The shape of the transducers can be described by a the function  $\phi(\mathbf{x})$  of the spatial coordinate  $\mathbf{x}$ .

$$\phi(\mathbf{x}) = \begin{cases} 1, & \text{if } \mathbf{x} \in \Omega_P \\ 0, & \text{if } \mathbf{x} \in \Omega - \Omega_P \end{cases} \quad (3)$$

It can be supposed that each piezo-patch is characterized by a single polarization and the following assumptions are made:

- "through-the-thickness" polarization, i.e.  $D_1 = D_2 = 0$ .

- "plain strain", i.e. strain in the  $x_3$ -coordinate is negligible. Therefore, the strain vector consists in  $\varepsilon = [\varepsilon_{11}, \varepsilon_{22}, \gamma_{12}]^T$ .

Under these assumptions, (1) can be re-written as:

$$D_3 = \phi(\mathbf{x}) \mathbf{b}^T \mathbf{D} = \phi(\mathbf{x}) \mathbf{b}^T [\mathbf{e}^\sigma \varepsilon + \varepsilon^\varepsilon \mathbf{E}] \quad (4)$$

where  $\mathbf{b} = [0, 0, 1]^T$ . As a consequence, the  $D_3$  component of the electric displacement field in (1) is:

$$D_3 = \phi(\mathbf{x}) \mathbf{b}^T [\mathbf{d}^\sigma \mathbf{C}^E \varepsilon + (\varepsilon^\sigma - \mathbf{d}^\sigma \mathbf{C}^E \mathbf{d}^{\sigma T}) \mathbf{E}] \quad (5)$$

In sensing mode, the piezo-transducer can be modeled as a ideal capacitor, assuming  $E_1 = E_2 = 0$  and the voltage varies linearly across the thickness ( $t_p$ ):

$$\mathbf{E} = \frac{V}{t_p} \mathbf{b} \quad (6)$$

By using (6), and integrating (5), the following equation for the measured voltage  $V$  can be derived:

$$V = \frac{t_p}{A_P [\mathbf{b}^T (\varepsilon^\sigma - \mathbf{d}^\sigma \mathbf{C}^E \mathbf{d}^{\sigma T}) \mathbf{b}]} \mathbf{b}^T \mathbf{d}^\sigma \mathbf{C}^E \int_{\Omega} \varepsilon \phi(\mathbf{x}) d\mathbf{x} \quad (7)$$

where  $A_P$  is the area of the piezo-patch.

The out-of-plane displacement of a wave propagating in the plate can be expressed as:

$$\mathbf{u}(\mathbf{x}, \omega) = \mathbf{U}_0(\omega) e^{-j\mathbf{k}_0(\omega) \cdot \mathbf{x}} \quad (8)$$

where  $\mathbf{U}_0(\omega)$  denotes the amplitude and the polarization of the wave at frequency  $\omega$ , and  $\mathbf{k}_0(\omega) = k_0(\omega) \mathbf{i}'_1 = k_0(\omega) (\cos \theta \mathbf{i}_1 + \sin \theta \mathbf{i}_2)$  is the considered wave vector at angle  $\theta$ . Assuming that the only strain component is given by:

$$\varepsilon_{1'1'} = \frac{du'_{1'}}{dx'_{1'}} = jU_{1'0}(\omega) k_0(\omega) e^{-jk_0(\omega)x'} \quad (9)$$

The strain in (7) can be written as:

$$\varepsilon = \varepsilon_{1'1'} \mathbf{r}(\theta) \quad (10)$$

where  $\mathbf{r}(\theta) = [\cos^2 \theta, \sin^2 \theta, 0]$ . Substituing Eqs. 10 and 9 into Eq. 7, the voltage  $V(\omega)$  becomes:

$$V_P(\omega) = jU_{1'0}(\omega) k_0(\omega) H_P(\theta) D_P(\omega, \theta) \quad (11)$$

where:

$$H_P(\theta) = \frac{t_p \mathbf{b}^T \mathbf{d}^\sigma \mathbf{C}^E \mathbf{r}(\theta)}{A_P [\mathbf{b}^T (\varepsilon^\sigma - \mathbf{d}^\sigma \mathbf{C}^E \mathbf{d}^{\sigma T}) \mathbf{b}]} \quad (12)$$

and

$$D_P(\mathbf{k}_0(\omega)) = \int_{-\infty}^{\infty} \int_{-\infty}^{\infty} e^{-j\mathbf{k}_0(\omega) \cdot \mathbf{x}} \phi_P(\mathbf{x}) d\mathbf{x} \quad (13)$$

define two different contributions to the frequency piezo-response. The first quantity,  $H_P(\theta)$ , is related only to the piezoelectric material properties. For the case of monolithic PZT, the quantity  $H_P$  can be assumed constant for the different direction  $\theta$ .

Conversely, the quantity  $D_P$  describes the effect of the transducer shaping in the wavenumber domain, since it depends on the function  $\phi_P(\mathbf{x})$ . Therefore,  $D_P$  determines the directional properties of the sensor. For this reason, it is referred to as *Directivity function*.

It is worth noting that the Directivity function can be seen as the 2D-Fourier Transform (2D-FT). Let us consider as an example a circular piezo-sensor of radius  $R$ , then (13) provides:

$$D_P(k_0, \theta) = 2\pi R^2 \frac{J_1(Rk_0(\omega))}{Rk_0(\omega)} \approx 2\pi R^2 \text{sinc}(Rk_0(\omega)) \quad (14)$$

where  $J_1(\cdot)$  is the first kind Bessel function of first order and  $k_0(\omega)$  is the wave vector of the propagation mode of Lamb waves (e.g., A0 or S0 mode). Observe that the function in (14) does not depend on  $\theta$ . Therefore, defining the sensor beampattern at frequency  $\omega$  as;

$$d(\omega, \theta) = \frac{|D_P(\omega, \theta)|}{\max_{\theta} [|D_P(\omega, \theta)|]} \quad (15)$$

it can be concluded that  $d(\omega, \theta) = 1$ . Alternatively, it is possible to design the transducer shape so that its beampattern is anisotropic and influenced by the actuated frequency, as discussed in the next Section.

### III. THE REALIZATION OF INHERENTLY DIRECTIONAL TRANSDUCERS

The key idea for the FSAT design stems from the invertibility of the Fourier transform: indeed, it is conceivable to impose an arbitrary Directivity function, and consequently the sensor beampattern, by determining the *shape function* from the inversion of (13), i.e.:

$$\phi_P(\mathbf{x}) = F^{-1} \{D_P(\mathbf{k}_0(\omega))\} \quad (16)$$

where  $F^{-1}$  denotes the Inverse bi-dimensional FT.

This idea was put in place for the first time by Senesi and Ruzzene in [9]. In this work, the Directivity function was designed so that at each excited frequency, the beampattern was oriented toward a specific direction or angle. This was achieved by designing the directivity function as a combination of multiple first order Bessel functions  $J_1(x)$  arranged on two symmetrical spirals (see figure 2):

$$D_P[k_0, \theta] = -j \frac{a}{N} \sum_{n=1}^N \left[ \frac{J_1(a|k_0 - k_n|)}{a|k_0 - k_n|} - \frac{J_1(a|k_0 + k_n|)}{a|k_0 + k_n|} \right] \quad (17)$$

where  $a$  is a spatial dimension and  $k_n$  is the wave vector associated with the angle  $\theta_n$ , according to the following relation:

$$k_n = [k_m + (k_M - k_m) \frac{\theta_n - \theta_m}{\theta_M - \theta_m}] (\cos \theta_n i_1 + \sin \theta_n i_2) \quad (18)$$

With this arrangement the peaks of the Bessel functions are spaced by constant arc-lengths throughout the spiral [10]. Therefore, increasing wavenumbers, and consequently frequencies, leads to beampatterns oriented at increasing angles  $\theta_n$ .

Note that the Directivity function in (17) is Hermitian with respect to the origin, i.e. its amplitude is symmetric and its phase is anti-symmetric. Such property is essential to generate a real shape function with the inverse Fourier Transform.

It is worth highlighting some important facts:

- **Finite extension of the transducers.** The superposition of Bessel functions in (17) is instrumental to generate shape functions with finite extension. More specifically, the spatial dimension  $a$  determines the radius of the transducer. However, Bessel functions have secondary maxima which generate detrimental sidelobes in the transducer beam pattern. Moreover, the smaller is  $a$ , the larger is the width of the main lobe. Therefore there is a trade-off involved between the transducer dimensions and their directivity.
- **Quantization of the shape function.** The inverse FT of the Directivity function is not necessarily a discrete function whose values are just 0s or 1s as requested from the definition in (3). Conversely, the inversion generates shape functions which are continuously modulated in amplitude and that can be positive or negative (or null). In [11], Senesi et al. achieved a feasible F-SAT by applying a binary quantization procedure to the shape function resulting from (16) so that all values higher than a positive threshold are set to 1, and all ones lower than a negative threshold are set to -1. Since it not conceivable to apply opposite polarities, this solution implies that the FSAT consists in two distinct patches (associated to the positive and negative values of the quantized shape function, respectively) whose signals (either actuated or received) must be considered in phase opposition.
- **Practical realization** The FSAT design concept was validated with different realizations. The first solutions presented in literature were based on metallized PVDF (polyvinylidene fluoride) sheets. The shaping of the electrodes on the upper surface can be achieved with a laser cut as in [12], [13]. Alternatively, metallic electrodes shape can be printed on PVDF films, as proposed in [6], or by using lithographic procedures as in [14].
- **Trading-off angular and radial resolutions** The design criterion may show some limitations in the damages detection and localization tasks. In fact, an intrinsic trade-off between the distance and angle estimation accuracy can be observed: due to the fact that the beam steering is obtained as a simple function of the excited frequency, the broader is the frequency content of the excited pulse the wider is the uncertainty for angle estimation. Vice-versa, the range evaluation requires broadband excitation signals to increase its estimation accuracy, as well known in Radar antennas Theory ([15]). Further details on this trade-off were analyzed in [16].

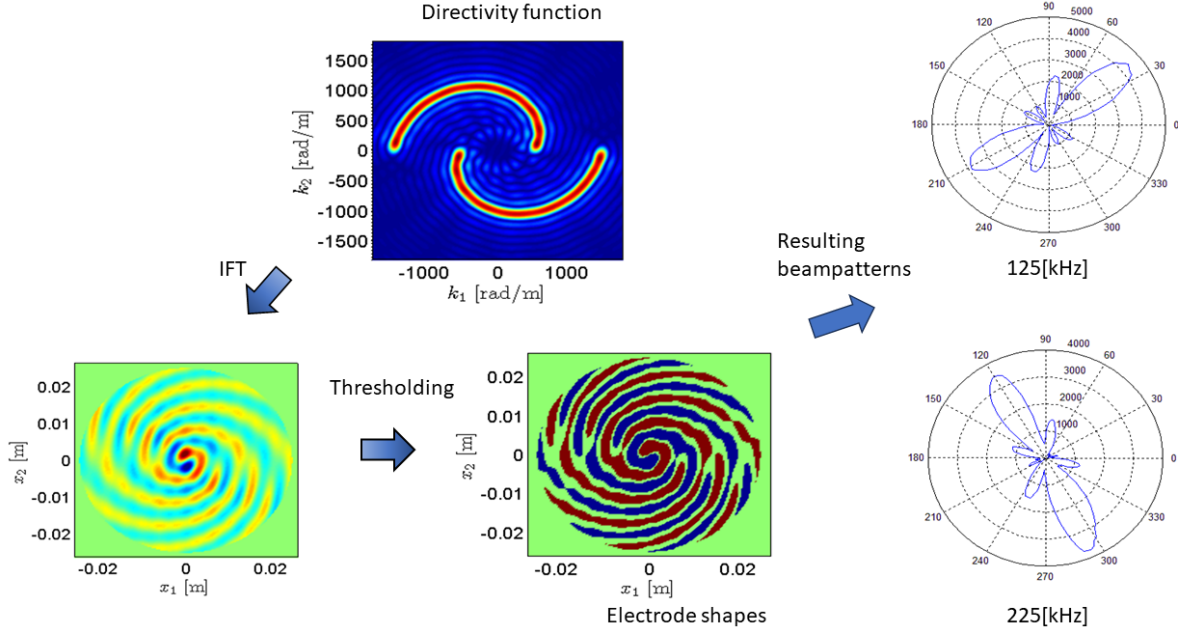


Fig. 2. Design procedure of FSAT, and beampattern achieved by actuating the transducer with monochromatic signals at different frequencies.

- **180° ambiguity** Finally, another important issue is related to the 180° ambiguity in the DoA estimation: due to the symmetry of the Directivity function it is impossible to determine whether a wave is received from angle  $\theta$  or  $\theta + 180^\circ$ . Similarly, in actuation, waves are transmitted simultaneously in opposite directions.

In the next Section, some possible modifications and extensions of the design procedure will be introduced to show how the mentioned limitations can be overcome.

#### IV. A NEW GENERATION OF FREQUENCY STEERABLE TRANSDUCERS

##### A. Unidirectional FSATs

A novel Sensor has been presented in [17] to detect guided waves propagating along a single direction, avoiding the 180° ambiguity.

Such result was achieved by subdividing the shape function in two parts, referred to as *real* ( $\phi_{ReP}(\mathbf{x})$ ) and *imaginary* ( $\phi_{ImP}(\mathbf{x})$ ). Let us suppose that both of them may generate waves along direction  $\mathbf{k} = \pm \mathbf{k}_c$ , so that:

$$\begin{aligned} F\{\phi_{ReP}(\mathbf{x})\} &\doteq D_R = \\ A_R (e^{j\varphi_1} \delta(\mathbf{k} + \mathbf{k}_c) + e^{-j\varphi_1} \delta(\mathbf{k} - \mathbf{k}_c)) \\ F\{\phi_{ImP}(\mathbf{x})\} &\doteq D_I = \\ A_I (e^{j\varphi_2} \delta(\mathbf{k} + \mathbf{k}_c) + e^{-j\varphi_2} \delta(\mathbf{k} - \mathbf{k}_c)) \end{aligned} \quad (19)$$

where  $A_R$ ,  $A_I$  and  $\varphi_1$ ,  $\varphi_2$ , are the amplitude and phases at  $\mathbf{k}_c$ , respectively.

Let us suppose to excite a cosine wave with a unitary amplitude on the real part with frequency  $\omega_c$ , corresponding to the  $\mathbf{k}_c$  value via the dispersion curve of a certain structure to be monitored. Then, let us suppose to apply on the imaginary part the same signal with a  $\pi/2$  phase shift. Such signals can be represented in the phase domain in this way:

$$\begin{aligned} U_R(\omega) &= \delta(\omega + \omega_c) e^{-j\varphi} + \delta(\omega - \omega_c) e^{+j\varphi} \\ U_I(\omega) &= -j\delta(\omega + \omega_c) e^{-j\varphi} + j\delta(\omega - \omega_c) e^{+j\varphi} \end{aligned} \quad (20)$$

By using the model in (11) for the piezo-sensor frequency response and, without lack of generality, discarding the constants and the known scale function factors (i.e  $\pm j$ ,  $k_0(\omega)$  and  $H_P(\theta)$ ), the frequency responses 11 for  $\omega > 0$  and  $\omega < 0$  are given by:

$$\begin{aligned} V_{P(\omega>0)}(\omega) &= U_{R(\omega>0)}(\omega) D_R(\mathbf{k}(\omega)) + U_{I(\omega>0)}(\omega) D_I(\mathbf{k}(\omega)) \\ V_{P(\omega<0)}(\omega) &= U_{R(\omega<0)}(\omega) D_R(\mathbf{k}(\omega)) + U_{I(\omega<0)}(\omega) D_I(\mathbf{k}(\omega)) \end{aligned} \quad (21)$$

Therefore:

$$\begin{aligned} V_P(\mathbf{k}, \omega) &= \\ &\left[ \begin{aligned} &A_R e^{j\varphi_1} (e^{-j\varphi_1} \delta(\mathbf{k} + \mathbf{k}_c) + e^{j\varphi_1} \delta(\mathbf{k} - \mathbf{k}_c)) \\ &+ j A_I e^{j\varphi_2} (e^{-j\varphi_2} \delta(\mathbf{k} + \mathbf{k}_c) + e^{j\varphi_2} \delta(\mathbf{k} - \mathbf{k}_c)) \end{aligned} \right] \cdot \\ &\cdot \delta(\omega - \omega_c) + \delta(\omega + \omega_c) \cdot \\ &\cdot \left[ \begin{aligned} &A_R e^{-j\varphi} (e^{-j\varphi_1} \delta(\mathbf{k} + \mathbf{k}_c) + e^{j\varphi_1} \delta(\mathbf{k} - \mathbf{k}_c)) \\ &- j A_I e^{-j\varphi} (e^{-j\varphi_2} \delta(\mathbf{k} + \mathbf{k}_c) + e^{j\varphi_2} \delta(\mathbf{k} - \mathbf{k}_c)) \end{aligned} \right] \end{aligned} \quad (22)$$

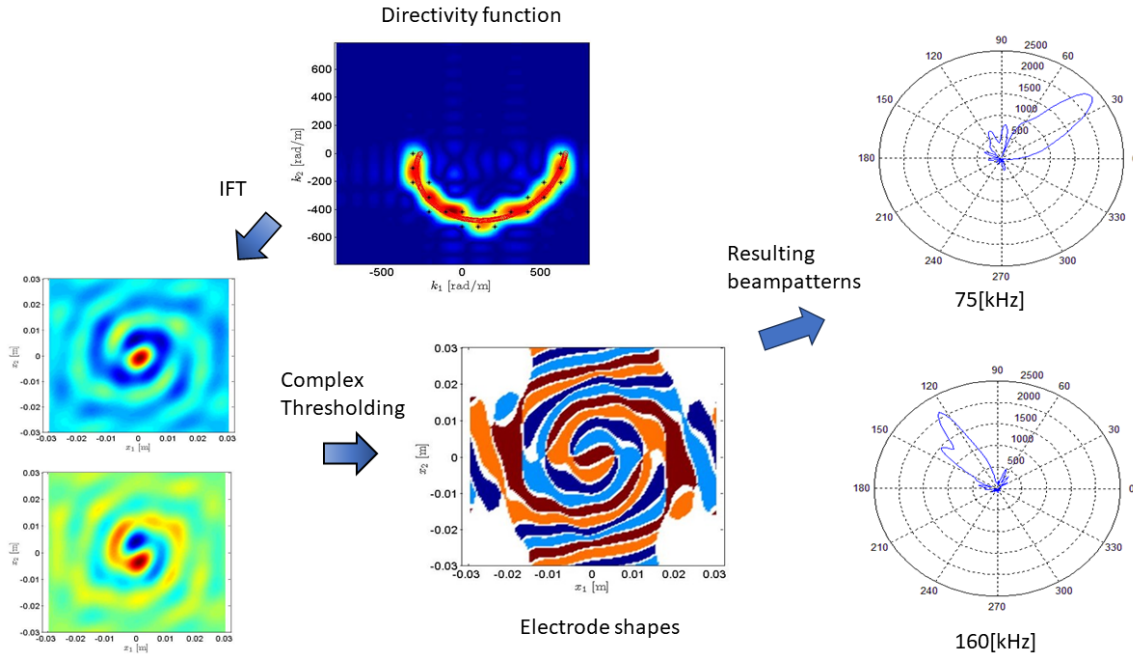


Fig. 3. Design procedure of an unidirectional FSAT, and beampattern achieved by actuating the transducer with monochromatic signals at different frequencies.

Finally, observe that if the two parts of the shape function,  $\phi_p(\mathbf{x})$ , are designed so that:

$$\begin{cases} A_R = A_I \\ \varphi_2 = \varphi_1 - \pi/2 \end{cases} \quad (23)$$

the  $\mathbf{k} - \omega$  response is Hermitian. The corresponding excited Lamb wave is given by:

$$\begin{aligned} V_p(\omega < 0)(\mathbf{k}, \omega) &= A_R e^{j(\varphi_1 + \varphi)} \delta(\mathbf{k} + \mathbf{k}_c) \delta(\omega + \omega_c) \\ V_p(\omega > 0)(\mathbf{k}, \omega) &= A_R e^{-j(\varphi_1 + \varphi)} \delta(\mathbf{k} - \mathbf{k}_c) \delta(\omega - \omega_c) \end{aligned} \quad (24)$$

which, indeed, corresponds to a unidirectional Lamb wave, excited in direction  $\mathbf{k}_c$ .

In essence, the two parts of the sensor are characterized by a phase shift equal to  $\pi/2$  in  $\mathbf{k}$ -space, an additional  $\pi/2$  shift is generated by the different actuations on the two parts, such that Lamb waves excited by the two parts interfere constructively and destructively in direction  $\mathbf{k}_c$  and  $-\mathbf{k}_c$ , respectively.

Taking into account that  $F^{-1}\delta(\mathbf{k} - \mathbf{k}_c) = e^{-j\mathbf{k}_c \cdot \mathbf{x}}$  a simple way to generate the two quadrature parts is to take the real and imaginary parts of  $e^{-j\mathbf{k}_c \cdot \mathbf{x}}$ . It is also worth noting that the implemented device can be used to sense unidirectionally the Lamb waves by applying a  $\pi/2$  phase shift to the signal acquired by the *imaginary* patch and then adding the signal acquired by the *real* patch.

The procedure illustrated for a single specific wavenumber ( $\mathbf{k}_c$ ) can be repeated to actuate multiple waves by: i) generating a suitable non-Hermitian Directivity function, ii) performing the Fourier inverse transformation and then generating the two parts from the real and imaginary components resulting from the anti-transformation.

Note that, the described procedure produces again continuously modulated shape functions for the two parts which must be quantized. A possible realization of this solution is presented in [18] (see Figure 3), in which the directivity function is designed in the following way:

$$D_P(\mathbf{k}) = \sum_{n=1}^N \text{Ker}(\mathbf{k}_n) \quad (25)$$

where  $\text{Ker}(\mathbf{k}_n)$  are Gaussian kernels centered in  $\mathbf{k}_n$  whose locations may be arranged as in (18).

The inverse transform emerges as a complex function  $\phi_p(x_1, x_2)$ , encompassing the real ( $Re$ ) and imaginary ( $Im$ ) parts. Employing complex thresholding of this function [19], the configuration of electrodes for the piezoelectric transducer can be determined. Each individual point within the spatial domain of  $\phi_p(x_1, x_2)$  is attributed to four distinct electrodes:

$$\bar{\phi}_p(x_1, x_2) = \begin{cases} E1 & \text{if } Re(\phi_p(x_1, x_2)) > |Im(\phi_p(x_1, x_2))| + \delta \\ E2 & \text{if } Re(\phi_p(x_1, x_2)) < -|Im(\phi_p(x_1, x_2))| - \delta \\ E3 & \text{if } Im(\phi_p(x_1, x_2)) > |Re(\phi_p(x_1, x_2))| + \delta \\ E4 & \text{if } Im(\phi_p(x_1, x_2)) < -|Re(\phi_p(x_1, x_2))| - \delta \end{cases} \quad (26)$$

where  $\delta$  represents an arbitrary positive value.

It is worth noting that, if we transform back in the wavenumber domain the quantized shaped function, the resulting function shows some deviation with respect to the original directivity function [6].

In order to address this problem, it is necessary to define a sensor shape function which is continuously modulated in its



values. Techniques developed in image processing to quantize grey scale images with a bit per pixel, can be fruitfully adopted for the transducer design purpose. In particular, the so called *half-toning* technique can be used (see [20], [21]) to modulate the piezoelectric load by properly patterning the metalization layers of the transducers [22], [17].

### B. Novel Solutions for the directivity function

As mentioned in Section II, a potential drawback of the spiral arrangement of the directivity function of FSATs is in the fact that signals actuated or sensed along a given direction are narrowband. However, the transducer design procedure described in the previous paragraphs is compatible also with different arrangements of the Directivity function. For example, in [17], we imposed the Directivity function (and so the same frequency response) of a piezo-disk in the  $[0-90]^\circ$  angular sector and 0 elsewhere. Then, via the 2D-Inverse FT (IFT), it is possible to obtain the shape function illustrated in Figure 4. The beampattern of this transducer generates and senses waves just in one quadrant.

Alternatively, in [23], a transducer capable of generating or sensing propagating waves along a reduced set of angles was proposed to minimize the effect of multi-path interference. In addition, three different Gaussian Kernels were defined at each chosen direction, in order to enlarge the available bandwidth of the signals which are transmitted or received along the different directions, allowing for enhanced versatility and flexibility in wave generation. The directivity function of such transducer, along with a photo of the transducer prototype and the related beampattern as a function of the actuated frequency, are depicted in Figure 5.

### C. Novel realizations based on PZT plates

In [24], an experimental validation of a shaped PZT transducer, obtained via the screen-printing technique, is provided. Piezoceramic transducers outperform those realized PVDF in terms of efficiency in guided wave actuation. Moreover, the screen printing applied to PZT plates allows the realization of electrodes characterized by very small spatial features (around  $200/250\ \mu\text{m}$ ), and, at the same time, to limit the manufacturing cost.

It is worth noting that, in the practical usage of these devices, it must be taken into account the effect of the transducer thickness (hence stiffness) and also the glue layer thickness [25] to properly predict how the radiation pattern is influenced by the spectral content of the actuated signal.

## V. CONCLUSIONS

A possible solution to tackle the complexity of beamforming based on phased arrays is in the shaping of the piezoelectric transducer electrodes to achieve the capability of steering the ultrasonic beam by simply controlling the central frequency of the actuated pulse.

Indeed, Frequency steerable transducers exploit the design of the directivity function to generate and receive waves along

different directions corresponding to the frequency of excitation/incoming wave. In this work, it has been discussed how the electrode shapes design methodology could be adapted to remove the  $180^\circ$  degrees ambiguity which characterizes the first realizations of the frequency steering concepts [6], and how the concept could be extended to transmit and sense wide band signals. The realization of the FSAT electrodes via half toning techniques may further improve the directivity of the implement transducers.

## ACKNOWLEDGMENT

The research described in this article was the result of collaborations spanning more than a decade with numerous researchers, among whom the authors would like to mention Massimo Ruzzene, Matteo Senesi, David Gottfried, Emanuele Baravelli, Alessandro Marzani, Antonio Palermo, Nicolò Speciale, Nicola Testoni, Federica Zonzini, Jochen Moll, Octavio Marquez-Reyes, Beata Zima and Sylvia Gebhardt.

## REFERENCES

- [1] Marilyne Philibert, Kui Yao, Matthieu Gresil, and Constantinos Soutis. Lamb waves-based technologies for structural health monitoring of composite structures for aircraft applications. *European Journal of Materials*, 2(1):436–474, 2022.
- [2] WAK Deutsch, A Cheng, and JD Achenbach. Self-focusing of rayleigh waves and lamb waves with a linear phased array. *Journal of Research in Nondestructive Evaluation*, 9(2):81–95, 1997.
- [3] Victor Giurgiutiu and Jingjing Bao. Embedded-ultrasonics structural radar for nondestructive evaluation of thin-wall structures. In *ASME International Mechanical Engineering Congress and Exposition*, volume 36258, pages 333–340, 2002.
- [4] Willi G Schwarz, Michael E Read, Matthew J Kremer, Mark K Hinders, and Barry T Smith. Lamb wave tomographic imaging system for aircraft structural health assessment. In *Nondestructive Evaluation of Aging Aircraft, Airports, and Aerospace Hardware III*, volume 3586, pages 292–296. SPIE, 1999.
- [5] Lingyu Yu and Victor Giurgiutiu. In situ 2-d piezoelectric wafer active sensors arrays for guided wave damage detection. *Ultrasonics*, 48(2):117–134, 2008.
- [6] Emanuele Baravelli, Matteo Senesi, David Gottfried, Luca De Marchi, and Massimo Ruzzene. Inkjet fabrication of spiral frequency-steerable acoustic transducers (fsats). In *Health Monitoring of Structural and Biological Systems 2012*, volume 8348, page 834817. International Society for Optics and Photonics, 2012.
- [7] Karl F Graff. *Wave motion in elastic solids*. Courier Corporation, 2012.
- [8] Victor Giurgiutiu and Adrian Cuc. Embedded non-destructive evaluation for structural health monitoring, damage detection, and failure prevention. *Shock and Vibration Digest*, 37(2):83, 2005.
- [9] Matteo Senesi and Massimo Ruzzene. A frequency selective acoustic transducer for directional lamb wave sensing. *The Journal of the Acoustical Society of America*, 130(4):1899–1907, 2011.
- [10] Emanuele Baravelli, Matteo Senesi, Massimo Ruzzene, Luca De Marchi, and Nicolò Speciale. Double-channel, frequency-steered acoustic transducer with 2-d imaging capabilities. *IEEE Transactions on Ultrasonics, Ferroelectrics, and Frequency Control*, 58(7):1430–1441, 2011.
- [11] Matteo Senesi, Emanuele Baravelli, Luca De Marchi, and Massimo Ruzzene. Experimental demonstration of directional GW generation through wavenumber-spiral frequency steerable acoustic actuators. In *2012 IEEE International Ultrasonics Symposium*, pages 2694–2697. IEEE, 2012.
- [12] Lorenzo Capineri, Alessandro Gallai, and Leonard Masotti. Design criteria and manufacturing technology of piezo-polymer transducer arrays for acoustic guided waves detection. In *2002 IEEE Ultrasonics Symposium, 2002. Proceedings.*, volume 1, pages 857–860. IEEE, 2002.



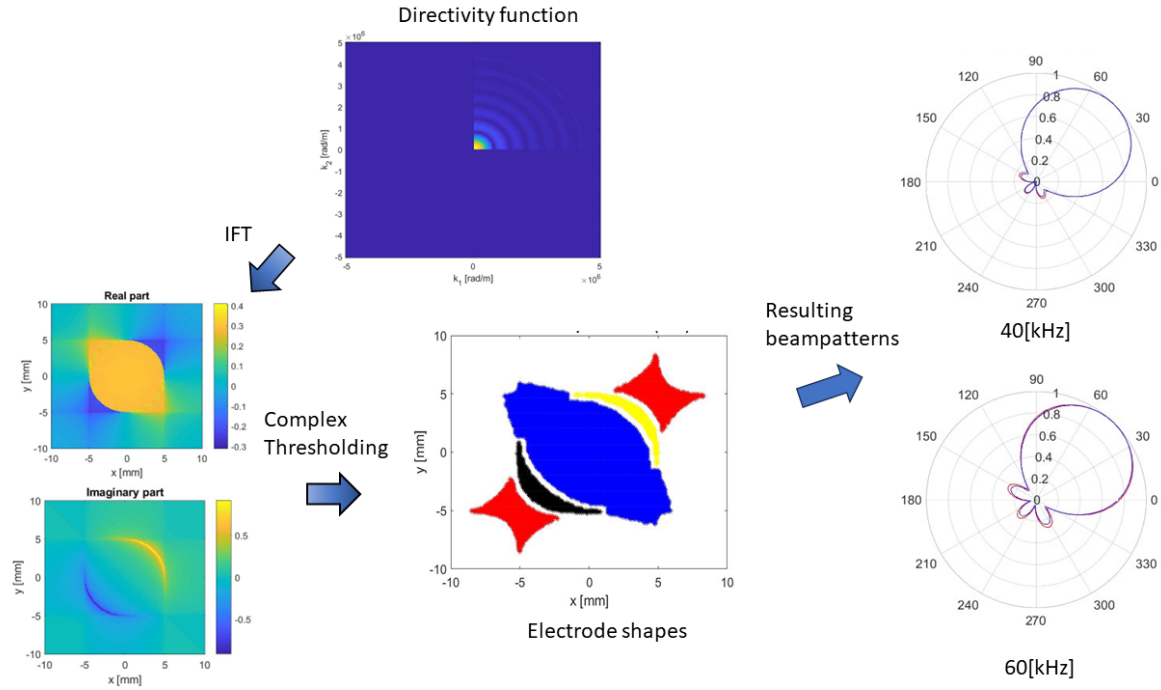


Fig. 4. Design procedure of a transducer having the same directivity function of a piezo-disk but just in the first quadrant [17], and beampatterns achieved by actuating the transducer with monochromatic signals at different frequencies.

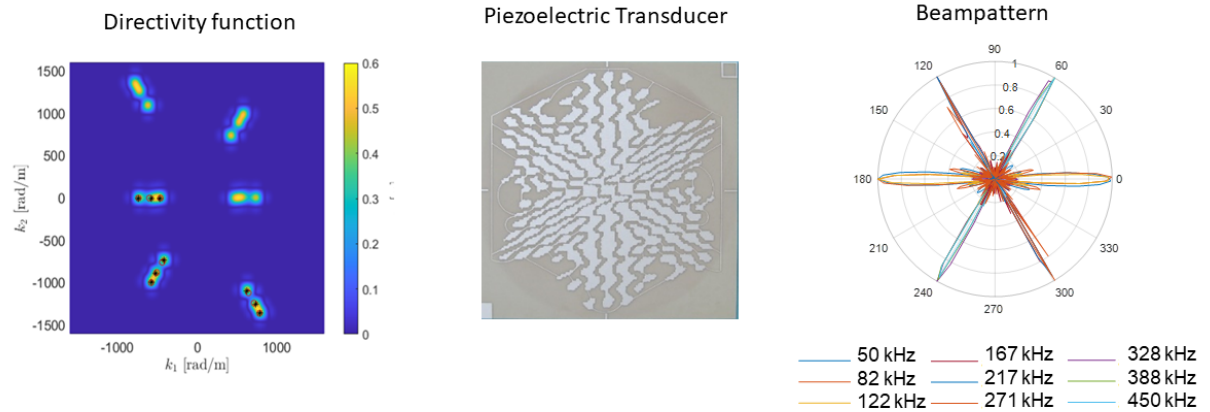


Fig. 5. Directivity function of a FSAT for Ultrasonic communications [23], a photograph of the manufactured device, and beampatterns achieved by actuating the transducer with monochromatic signals at different frequencies.

- [13] Filippo Bellan, Andrea Bulletti, Lorenzo Capineri, Leonardo Masotti, Goksen G Yaralioglu, F Levent Degertekin, BT Khuri-Yakub, Francesco Guasti, and Edgardo Rosi. A new design and manufacturing process for embedded lamb waves interdigital transducers based on piezopolymer film. *Sensors and Actuators A: Physical*, 123:379–387, 2005.
- [14] Emanuele Baravelli, Matteo Senesi, Massimo Ruzzene, and Luca De Marchi. Fabrication and characterization of a wavenumber-spiral frequency-steerable acoustic transducer for source localization in plate structures. *IEEE Transactions on Instrumentation and Measurement*, 62(8):2197–2204, 2013.
- [15] M.I. Skolnik. *Introduction to Radar Systems*. Electrical engineering series. McGraw-Hill, 2001.
- [16] Octavio A Márquez Reyes, Beata Zima, Jochen Moll, Masoud Mohammadgholiha, and Luca De Marchi. A numerical study on baseline-free damage detection using frequency steerable acoustic transducers. In *European Workshop on Structural Health Monitoring*, pages 24–33. Springer, 2023.
- [17] Marco Dibiase, Masoud Mohammadgholiha, and Luca De Marchi. Optimal array design and directive sensors for guided waves doa estimation. *Sensors*, 22(3):780, 2022.
- [18] Masoud Mohammadgholiha, Jochen Moll, and Luca De Marchi. A new generation of piezoceramic frequency steerable acoustic transducers for the rapid inspection of large areas of metallic plate structures. In *2023 IEEE International Ultrasonics Symposium*. IEEE, 2023.
- [19] Luca De Marchi, Nicola Testoni, and Alessandro Marzani. A new generation of frequency steerable transducers for lamb waves inspections. *e-Journal of Nondestructive Testing*, 21(7):1–8, 2016. 19th World Conference on Non-Destructive Testing (WCNDT 2016), 13-17 June 2016 in Munich, Germany.
- [20] Thomas D Kite, Brian L Evans, and Alan C Bovik. Modeling and

- quality assessment of halftoning by error diffusion. *IEEE Transactions on Image Processing*, 9(5):909–922, 2000.
- [21] Daniel L Lau, Gonzalo R Arce, and Neal C Gallagher. Green-noise digital halftoning. *Proceedings of the IEEE*, 86(12):2424–2444, 1998.
  - [22] Luca De Marchi, Nicola Testoni, and Alessandro Marzani. Device, method and system for real time structural diagnostics with guided elastic waves, February 9 2021. US Patent 10,914,711.
  - [23] Masoud Mohammadgholiha, Federica Zonzini, Jochen Moll, and Luca De Marchi. Directional multi-frequency guided waves communications using discrete frequency-steerable acoustic transducers. *IEEE Transactions on Ultrasonics, Ferroelectrics, and Frequency Control*, pages 1–1, 2023.
  - [24] Masoud Mohammadgholiha, Antonio Palermo, Nicola Testoni, Jochen Moll, and Luca De Marchi. Finite element modeling and experimental characterization of piezoceramic frequency steerable acoustic transducers. *IEEE Sensors Journal*, 22(14):13958–13970, 2022.
  - [25] Victor Giurgiutiu. Tuned lamb wave excitation and detection with piezoelectric wafer active sensors for structural health monitoring. *Journal of intelligent material systems and structures*, 16(4):291–305, 2005.